universität wien

DIPLOMARBEIT

Titel der Diplomarbeit

Raman microscopy and ecological stoichiometry: Opening the black box of the microbial cell

angestrebter akademischer Grad

Magister der Naturwissenschaften (Mag. rer. nat.)

Verfasserin / Verfasser:	Marvin Pölzl
Matrikel-Nummer:	0204265
Studienrichtung /Studienzweig (lt. Studienblatt):	Ökologie
Betreuerin / Betreuer:	Doz. Mag. Dr. Tom J. Battin

Wien, im Jänner 2009

Abstract

Ecological stoichiometry presents a conceptual framework to describe the balance of multiple chemical elements in ecological interrelations. Sterner & Elser (2002) developed ideas to connect an organism's physiology with its elemental constitution, basically focusing on the relative composition of C, N and P. To dissect complex relationships of diverse community structures, I started to examine the influences of variable resource stoichiometry (C:N:P) on the macromolecular composition of a single bacterial strain of *Verrucomicrobium spinosum.* I suggest a novel approach based on measuring macromolecular constituents on a cellular level using Raman microspectroscopy. The advantages of this are manifold. The technique enabled detailed insight into the connections between external C, N and P resources and their allocation in cellular biomolecules, such as carbohydrates, proteins and nucleic acids.

For this work, I used *V. spinosum* from batch cultures with 12 different resource stoichiometries (CNP). Bacterial cells were harvested during logarithmic and stationary growth to examine growth-dependent (physiological) influences on the intracellular composition. Analyses revealed clear physiological constraints in the logarithmic phase and a higher degree of heterogeneity in the stationary phase. Furthermore, I found good correlations between Raman-derived cell-level results on carbohydrates, proteins and nucleic acids and bulk biomass CNP using traditional chemical analysis.

Principal component analysis revealed substantial influences of N and P on the accumulation of the cellular constituents whereas the C supply apparently did not affect the assembly of carbohydrates, since also the low concentration level offered a surplus of C resources. In conclusion, this cell-level approach provides a valuable improvement of the accessibility of how resource stoichiometry affects microbial stoichiometry.

Introduction

The conceptual framework of ecological stoichiometry (Sterner & Elser 2002) utilizes chemical elements primarily considering elemental ratios to describe ecological interactions and fluxes from single organisms to higher trophic levels and whole ecosystems. These applications also imply studies of nutrient recycling, resource competition, growth and nutrient limitation patterns. Sterner and Elser (2002) connected biological function and elemental composition since dominant classes of organic macromolecules such as proteins, nucleic acids, lipids and carbohydrates differ substantially in their contribution of carbon, nitrogen and phosphorus, three of the main components in structural molecules. The chemical composition of organisms varies among species and is controlled by their physiology. Consequentially, different biological functions and life strategies are associated with diverse biochemical and elemental demands. For instance, this was applied in the idea of the growth rate hypothesis, which proposes a positive linear relationship between the growth rate and the ribosomal RNA (rRNA). The rRNA contains a large fraction of the cells P-content and therefore growth rate could also be coupled to the organism's phosphorus concentration. This is one example where ecological stoichiometry specified linkages between elemental and macromolecular composition and the physiology of organisms.

Heterotrophic bacteria play a crucial role as a decomposing compartment in terrestrial and aquatic ecosystems. The C:N ratios of the available detritus and of the microbial decomposers themselves often determine the rate of mineralization through affecting the N-specific uptake rate and carbon use-efficiency (Dodds et al. 2004, Manzoni et al. 2008). Improvements in identifying intracellular resource allocation by tracking substrate concentrations to particular macromolecular pools could help to understand the dependence of a decomposers physiology to resource stoichiometry.

In this study, I address the degree of homeostasis governed by intracellular composition of macromolecules, which might alternate between different growth conditions. Homeostasis realized as a physiological ability to maintain a constant macromolecular composition within a biologically defined range. It was already revealed that single bacterial species (e.g. *Escherichia coli*) grown at different C:N:P ratios tend to be subject to strict constraints and therefore are strongly homeostatic in terms of elemental composition (Makino et al. 2003). This study on *E. coli* indicated that varying supply C:P ratio has just minor influence on the

biomass P content but varied most as a function of varying growth rate and therefore its varying rRNA content. *E. coli* grown in a wide range of resource C:N:P ratios produced a much smaller variation of biomass C:N:P. Therefore, Makino et al. (2003) proposed that the regulation of the elemental composition of individual bacterial strains is firmly restricted to characteristic biomass C:N:P ratios and they thus are stoichiometrically homeostatic. This lead to the assumption that the observed variation in biomass C:N:P of bacterial freshwater communities (Tezuka 1990) may be due to dominance shifts of different strains. In conclusion, analyzing bulk biomass might not reveal sufficient specific information because both communities and mono-species cultures imply a heterogeneous composition of physiological modes and states what might create masking issues on the actual effects of resource stoichiometry on a cells metabolism.

Therefore, the intention of this survey was not to focus on bulk communities but to divide the community structure into its units and to face a single bacterial species at single-cell level.

For a long time, Raman spectroscopy has been a common and well-established tool in the chemical industry and medical research (Goodacre et al. 1998, Schrader et al. 1999, Hanlon et al. 2000). At the same time, it demonstrated its advantages in the extraction of biochemical information from microbiological samples (Naumann et al. 1995) especially because of its applicability on objects at a micro-scale resolution.

As photons interact through inelastically scattering with all available intracellular molecular constituents, an acquired Raman spectrum contains cumulative multidimensional information on the chemical composition of all cell components (Schuster et al. 2000) and is therefore mainly utilized as a whole-cell fingerprinting technique. Besides, it is a preferred solution if a non-destructive or even non-invasive and rapid method is required. There is also just little interference of water and often scarce volumes of samples are sufficient and measurable. Raman spectroscopy applied on bacteria was elaborated to function as an identification procedure based on differences in the spectral patterns caused by varying complexity of the intracellular composition of macromolecular constituents (Huang et al. 2004). The results of various studies point out the high discriminatory power of the Raman technique that provides accurate differentiation of even closely related bacterial species (Kirschner et al. 2001, Lopez-Diez & Goodacre 2004). The identification potential within phylogenetically homogeneous bacterial groups (Jarvis & Goodacre 2004, Hutsebaut et al.

2006, Oust et al. 2006) and the possibility to even differentiate between physiological states (Escoriza et al. 2006) and growth stages (De Gelder et al. 2007a) of a single bacterial strain gave rise to the main questions of this study.

I applied Raman spectroscopy to the study of microbial stoichiometry and specifically devised several questions concerning the effects of varying nutrient supply on an individual bacterial species with perspectives to facilitate understanding of the transition from abiotic resources to intracellular macromolecules. This may help understand nutritional quality controlling the microbial physiology and in addition possible influences on complex food webs and broad-scale ecosystem processes such as carbon (Hessen et al. 2004) and nitrogen cycles.

Since it is proven that bacteria are homeostatic concerning their biomass stoichiometry this study was intended to ascertain resource- and growth-dependent variance in the macromolecular constitution of bacterial biomass. To be more explicit, I asked how different growth phases and variation in resource stoichiometry affect the macromolecular composition of the single bacterial strain *Verrucomicrobium spinosum*. As macromolecular compounds consist generally but in unequal parts of C, N and P, I attempted to link changes in the macromolecular composition to the respective biomass C:N:P ratio. Raman spectroscopy promised to be helpful for this purpose. Furthermore, I compared the results of the Raman measurements to traditional wet-chemical analyses of nucleic acids, carbohydrates and proteins.

To address these questions, the experimental setup was designed to deliver a broad range of varying CNP ratios and concentrations comprising the motive to force the strain towards the borders of limitation. Growing *V. spinosum* in batch-cultures allowed harvesting the strain in active (logarithmic) growth phase and in stationary phase reflecting different metabolic states.

Material & Methods

Cultivation

The reference strain *V. spinosum* (phylum *Verrucomicrobia*; ATCC 43997^T, IFAM 1439^T, DSM 4136^T) was obtained from DSMZ (Deutsche Sammlung von Mikroorganismen und Zellkulturen) as dried culture and transferred to glycerol stocks for storage (-80°C). *V. spinosum* is a gram-negative, heterotrophic and non-motile, rod-shaped bacterium with facultative anaerobic metabolism which was first detected in eutrophic lakes (Schlesner 1987), and is routinely identified in a variety of aquatic and terrestrial ecosystems.

Cells of *V. spinosum* were first streaked on solid agar plates of complex medium 607:M13 (Schlesner 1994) containing 1.5% Agar and grown at 30°C for up to 5 days before the plates were stored at 4°C. For subsequent experiments, the formula of the applied complex medium was modified in order to manipulate the C:N:P ratio by replacing the molybdenum source $(NH_4)_6MoO_7O_{24}$ with Na_2MoO_4 and $Co(NO_3)_2$ with $CoSO_4$ as cobalt source. Besides, we excluded compounds containing additional sources of C, N and P such as peptone, yeast extract, glucose and the vitamin solution.

Starter cultures were grown in aliquots of 50 mL liquid minimal medium in 250 mL Erlenmeyer flasks with 25 mM Glucose, 2.5 mM $NaNO_3$ and 0.25 mM Na_2HPO_4 by inoculating with approximately 20 cm of colony from the agar plates and incubating at 30°C for 67 hours until cell density reached an OD_{450} value of 0.4. Cultures were then harvested by centrifuging in Greiner tubes at 10800 x g for 15 min. The pellets of several tubes were combined and resuspended in minimal medium without C, N and P amendments and merged in order to ensure a uniform inoculum for all treatments in the main experiment. After washing and merging the pellets the biomass was resuspended in 12 mL of minimal medium of which two mL were used to inoculate one 2 L Erlenmeyer flask containing 400 mL of medium of the appropriate treatment. Consequently, the biomass of 50 mL pre-culture was adequate for six replicates.

Resource treatments consisted of C ($C_6H_{12}O_6$) added at two concentrations, each level of C had three levels of N ($NaNO_3$) while each level of N had two levels of P (Na_2HPO_4) resulting in a total of 12 unique C:N:P treatments (Table 1). For each resource treatment, cultures were grown in quadruplicate flasks, of which one was frequently subsampled to closely follow

population growth. Cultures were maintained at 22°C +/- 2°C while shaking on orbital shakers at 150 rpm.

Table 1: C, N and P concentrations and resource ratios for each resource treatment

	Concentrations			Ratios		
Treatment	**C [mM]**	**N [mM]**	**P [mM]**	**C:N**	**C:P**	**N:P**
1	150	12.5	0.25	12	600	50
2	150	12.5	0.025	12	6000	500
3	150	1.25	0.25	120	600	5
4	150	1.25	0.025	120	6000	50
5	150	0.125	0.25	1200	600	0.5
6	150	0.125	0.025	1200	6000	5
7	30	5	0.1	6	300	50
8	30	5	0.01	6	3000	500
9	30	0.5	0.1	60	300	5
10	30	0.5	0.01	60	3000	50
11	30	0.05	0.1	600	300	0.5
12	30	0.05	0.01	600	3000	5

Growth curves and harvesting points

In order to assess differences between physiological states of different growth stages cultures were harvested in logarithmic and stationary phase. The timings of logarithmic and stationary phase were determined *a priori* performing pre-experiments for each of the twelve treatments under the same conditions as in the main experiment but sub-samples were taken regularly to estimate cell density by measuring OD_{450} values. Based on the acquired data, logistic growth models were generated for each resource treatment using the following equation:

$$N(t) = \frac{k}{1 + (\frac{k-n}{n}) \times e^{(-r \times t)}}$$

where k is carrying capacity, n is number of cells, r is the intrinsic growth rate and t is time. Parameters k, n and r were estimated using the software Delta Graph which applies an iterative algorithm following the Levenberg-Marquardt method (Red Rock Software Inc.). Harvesting points were defined as $t = k/2$ for log phase and $t = k$ for stationary phase +/- 2 hours.

Cultures were harvested by centrifuging the entire 400 mL at 16,900 x g for 45 min. After discarding the supernatant the biomass pellet was washed with 50 mL 130 mM NaCl, vortexed and centrifuged again at 36,700 x g for 15 min and finally resuspended in 130 mM NaCl. An aliquot of 200 – 500 µL, depending on cell density, of the suspension was taken for fixation with paraformaldehyde, at a final concentration of 4%. Following the fixation in PFA for two hours at 4°C the cells were washed with PBS and later transferred to 300 – 800 µL of a 1:1 (vol:vol) mixture of 96% ethanol and PBS. Samples were stored at -20°C until they were analyzed by Raman spectroscopy. This procedure of sample preparation resulted in high quality Raman spectra for all resource treatments.

Raman spectroscopy

For Raman analysis, 1-2 µL of the fixed cell suspension was dried at 46°C on a calcium fluoride slide, which was used because of its low background signal in the appropriate wave-number range. Salt crystals were removed by briefly dipping the slide into Milli-Q ultrapure water and subsequent drying under a compressed air jet. Raman spectra of 20 randomly chosen individual cells were obtained using a LabRAM HR800 high resolution confocal Raman microscope (HORIBA Jobin-Yvon, UK) with an attached Olympus BX-41 microscope. Raman scattering was excited using a frequency doubled, diode pumped Nd:YAG laser with an excitation wavelength of 532.09 nm and a laser power of approximately 5-8 mW by using a density filter with an attenuation factor of 4. The background signal of the carrier material could be reduced by adjusting the confocal pinhole of the Peltier air-cooled CCD detector (open electrode format) to 250 µm and the slit size to 1000 µm. For the acquisition of the spectra a grating of 600 lines mm^{-1} (blazed at 500 nm) was utilized while recording with an accumulation time of 40 s to improve the signal-to-noise ratio. These settings were chosen to facilitate a spatial resolution of approximately 1 µm. The laser beam was centered visually on each cell and focused manually using a 100x/0.90 air objective. The Raman signal was collected in a spectral range of 380-2030 cm^{-1} but was reduced to an interval of 400-1780 cm^{-1} with an achieved average spectral resolution of 1.6 cm^{-1}. Recording of the spectra was accomplished using Labspec Raman Spectroscopy Software (Version 5.25.15, HORIBA Jobin-Yvon). The spectra were pre-processed before the data was further analyzed with Excel (Microsoft) and examined using statistical software. This pre-processing implied automatic

baseline correction, normalization and smoothing algorithms provided in the Labspec Software.

Principal component analysis (PCA) implemented in SPSS (Version 15) was applied on selected spectral data in order to discriminate between growth stages and treatments at different resource levels. Significant differences between found groupings were analyzed performing Mann-Whitney U-test (for two independent samples) and Kruskal-Wallis H-test (for k independent samples).

Bulk chemical analyses

The total carbohydrate content of the bacterial biomass was measured on lyophilized cell pellets using the Phenol assay (Daniels et al. 2007) due to a colorimetric reaction of carbohydrates with phenol in concentrated sulphuric acid. The total protein concentration was determined by incubating a sonicated cell suspension with an amino group binding dye (Coomassie Blue G) and subsequent spectrophotometric analysis (Bradford 1976). The total nucleic acid content was quantified by measuring the fluorescent signal after staining the sonicated cell suspension with RiboGreen® (Makino & Cotner 2004).

Total elemental phosphorus content of the bacterial biomass was ascertained through acid extraction with HNO_3 (65%) and $HClO_4$ (70%) and subsequent photometric measurement of the extinction at 882 nm (Schinner et al. 1993). Total elemental nitrogen and carbon content of lyophilized biomass was measured using an elemental analyzer (EA1110, CE Instruments, Milan, Italy) interfaced via a ConFlo II device (Finnigan MAT, Bremen, Germany) to a continuous-flow stable isotope ratio mass spectrometer (Delta Plus, Finnigan MAT, Bremen, Germany) (McKee et al. 2002, Watzka et al. 2006).

Results

Raman microspectroscopy was observed to provide detailed information about the macromolecular constituents by delivering reproducible vibrational spectra of single cells of the bacterial strain *V. spinosum*. Several cellular compounds could be assigned to distinct peaks located in the spectra such as nucleic acids, carbohydrates, lipids and proteins (Table 2, Figure 1). Some of these major constituents showed considerable changes between spectra found in logarithmic growth phase and stationary phase. In particular, peaks assigned to storage polysaccharides and carbohydrates rose whereas proteins, nucleic acid and lipid peaks demonstrate both rises and declines.

Table 2: Observed Raman bands in spectra of analyzed cells and tentative assignations

Wavenumber [cm^{-1}]	**Code**	**Assignment**	**Reference**
440	ca_1	carbohydrates	De Gelder et al. 2007
481	ca_2	carbohydrates	De Gelder et al. 2007; Goral & Zichy 1990
665	na_1	nucleic acids (guanine)	De Gelder et al. 2007; Maquelin et al. 2002
723	na_2	nucleic acids (adenine)	De Gelder et al. 2007; Maquelin et al. 2002
785	na_3	nucleic acids (cytosine, uracil)	De Gelder et al. 2007; Maquelin et al. 2002
854	ca_3	carbohydrates	De Gelder et al. 2007
936	ca_4	carbohydrates	De Gelder et al. 2007
1004	pr_1	phenylalanine (in proteins)	De Gelder et al. 2007
1030-1130	ca_5, ca_6, ca_7, ca_8	carbohydrates, mainly -C-C- (skeletal)	Schuster et al. 2000
1254	pr_2	proteins (amide III)	Maquelin et al. 2002
1338	pr_3	proteins	Kneipp et al. 2006
1450	li_1	lipids	Kneipp et al. 2006
1575	na_4	nucleic acids (guanine, adenine)	De Gelder et al. 2007; Maquelin et al. 2002
1660-1670	pr_4	proteins (amide I)	Maquelin et al. 2002

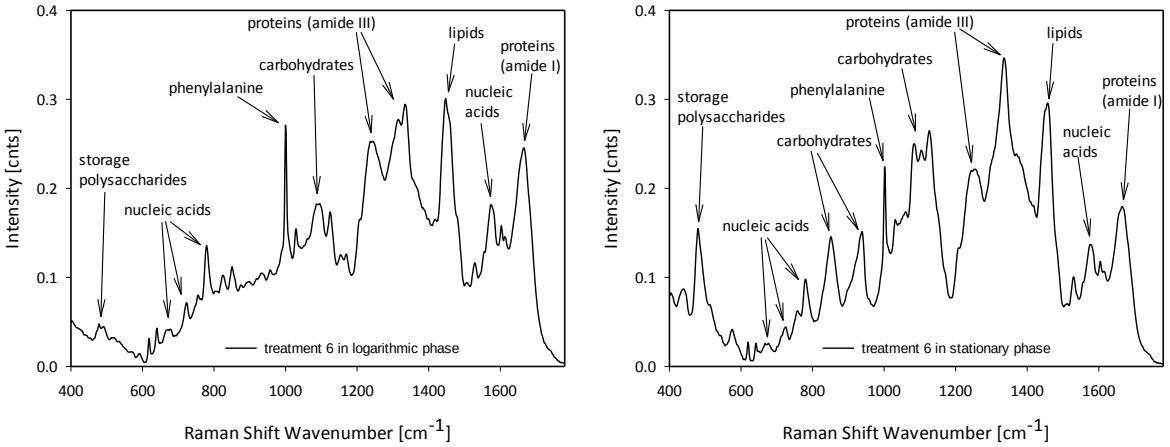

Figure 1: Exemplary spectra indicative of typical logarithmic (left) and stationary phase (right) spectra, including tentative peak assignments

In order to investigate the match of single-cell level Raman measurements with traditional bulk, chemical methods, data from both approaches were compared (Figures 2 to 4). As there exist several peaks assigned to the same compound in one spectrum, one total value for each compound was calculated by summing the respective individual peak intensities. The results indicate a significant positive correlation for carbohydrates (R^2 = 0.38, P < 0.01; Figure 2) and proteins (R^2 = 0.42, P < 0.001; Figure 3). In contrast, the relationship for nucleic acids was not significant when including both logarithmic and stationary phases. However, separating both growth phases revealed a significant positive correlation only for the logarithmic phase (R^2 = 0.55, P < 0.05; Figure 4). No correlation could be detected for the stationary phase (R^2 = 0.009, P = 0.74).

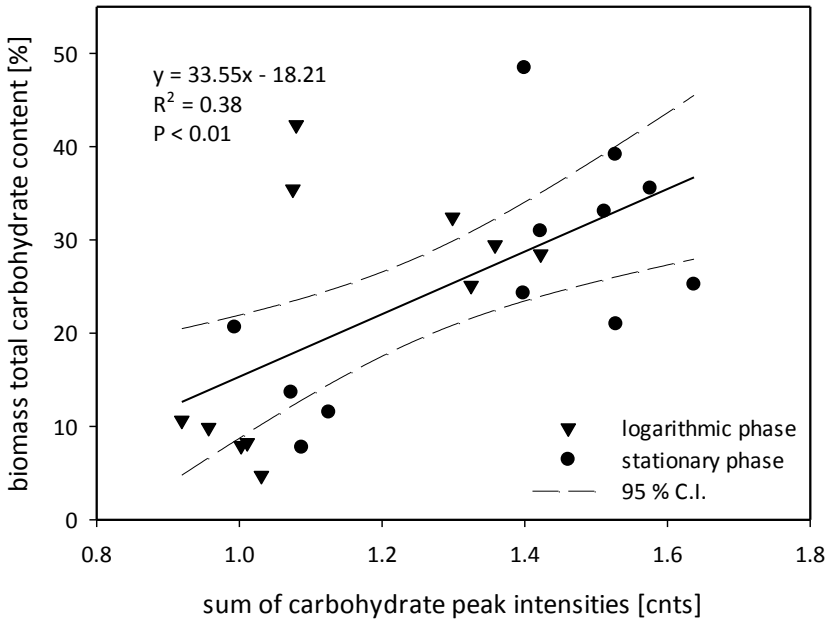

Figure 2: Relationship between total carbohydrate content [% of biomass] and sum of carbohydrate peak intensities, including samples of both logarithmic and stationary growth phase

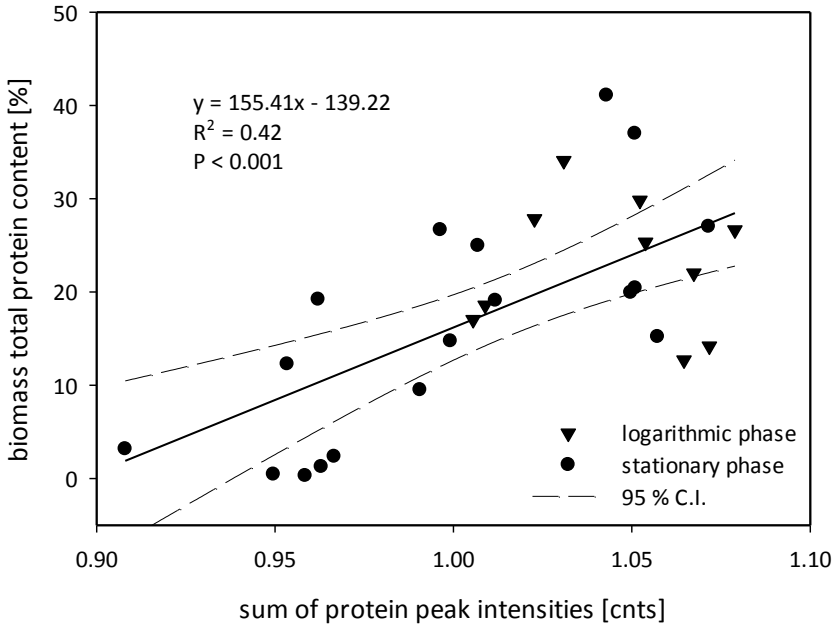

Figure 3: Comparison of total protein content [% of biomass] measured by traditional chemical methods with detected Raman peak intensities, including logarithmic and stationary phase samples

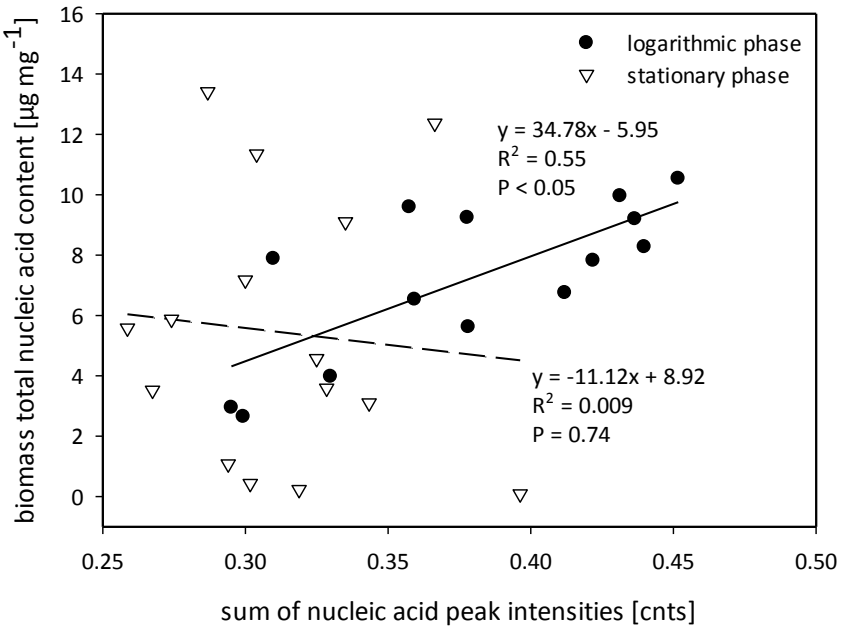

Figure 4: Correlation between fluorometric measured total nucleic acid content (µg per mg freshmass) and summarized nucleic acid peak intensities, for each growth stage separately

Besides, elemental concentrations were measured in bulk biomass. Calculated ratios could then be used for determining dependencies between the elemental composition of the biomass and the major macromolecular compounds containing these elements.

Figure 5 reveals a significant positive relationship between the C:N ratio and increasing carbohydrate peaks of the Raman spectra ($R^2 = 0.77$, $P < 0.0001$).

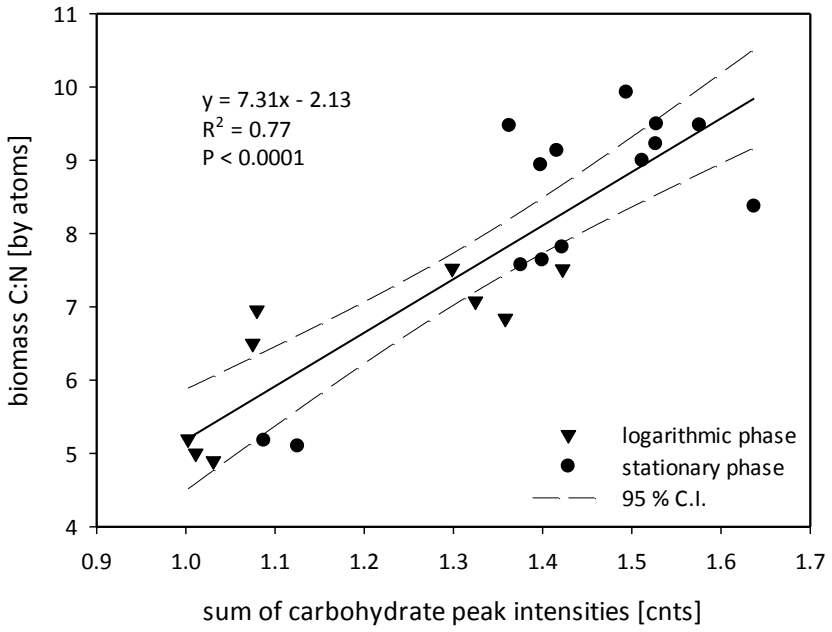

Figure 5: Relationship between biomass C:N ratio on total carbohydrate peak intensities measured through Raman spectroscopy, including samples of logarithmic and stationary growth phase

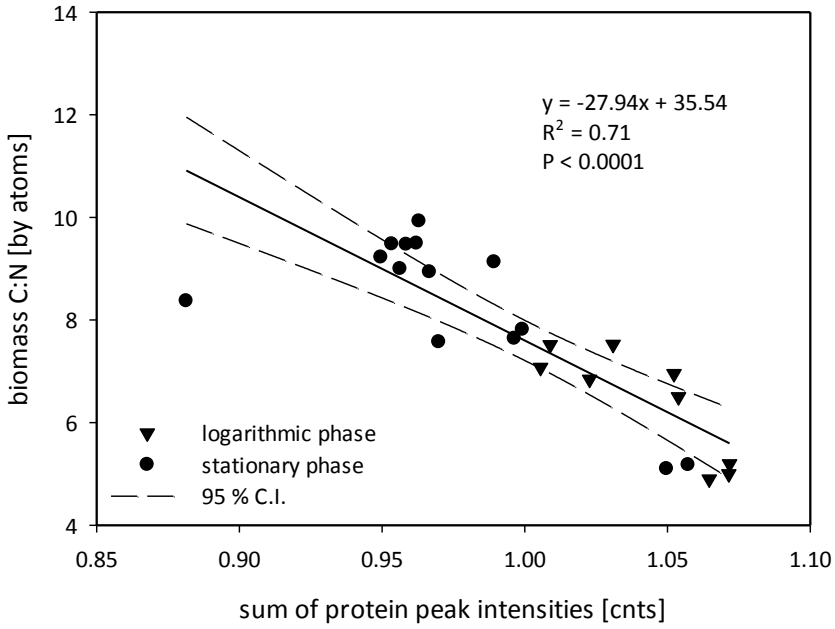

Figure 6: Relationship between biomass C:N ratio on cellular protein level measured through Raman spectroscopy, including samples of logarithmic and stationary growth phase

Raman protein peaks were inversely related to the C:N ratio of the bulk biomass (Figure 6).

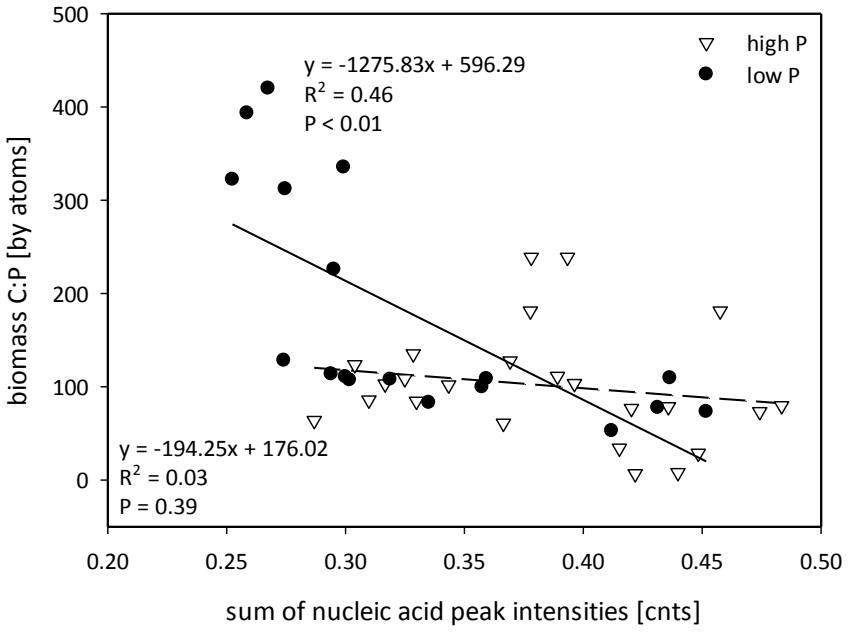

Figure 7: Relationship between biomass C:P ratio and total nucleic acid peak intensities measured through Raman spectroscopy, for high phosphorus separated from low phosphorus treatments

Since nucleic acids contain P, it is reasonable to explore possible relationships between Raman nucleic acid peaks and C:P ratios. Such a relationship existed for treatments containing low quantities of P ($R^2 = 0.46$, $P < 0.01$) but not for high P-treatments ($R^2 = 0.03$, $P = 0.39$) (Figure 7).

Multivariate analysis

The following multivariate statistics were based on 17 selected peaks (Table 2) which could be definitely identified and might imply considerable information.

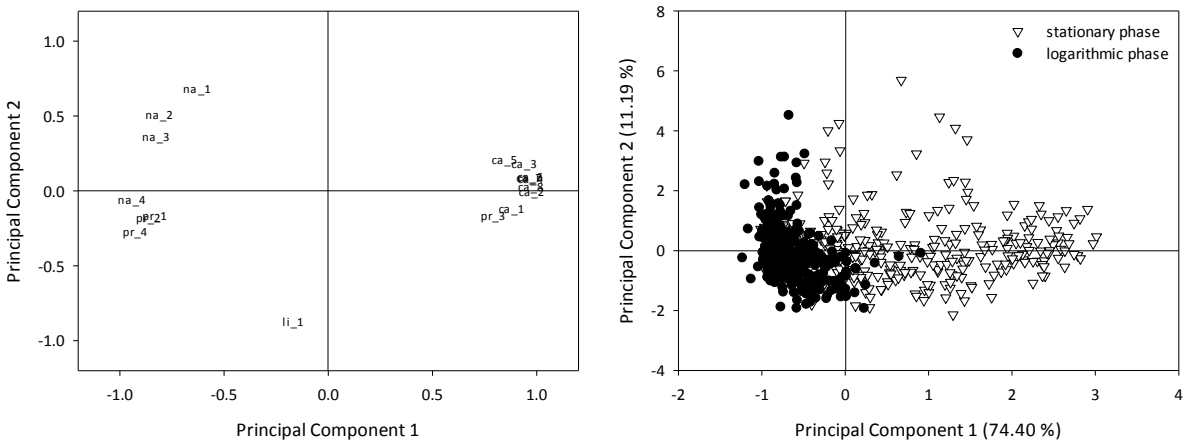

Figure 8: Loading plot (left) and score plot (right) for the first two components of a principal component analysis of logarithmic and stationary phase spectra, each symbol represents one measured spectrum

PCA with spectra of both growth phases (Figure 8) revealed a distinct separation of the logarithmic and stationary phase but a slight overlap on the negative side of PC1. In this case PC1 accounted for 74.4% and PC2 for 11.2% of the overall spectral variation.

The more scattered distribution of the stationary phase cluster indicates a higher degree of heterogeneity of that growth stage. The high degree of conformity of the logarithmic phase spectra was also noticeable in comparisons of spectra representing the 11 different treatments from the same growth stage (data and plots not shown). This comparison confirmed that spectral patterns were more variable in stationary phase.

Table 3: Results of Mann-Whitney U-Test for assessing possible significant differences between logarithmic and stationary phase spectra of all treatments at each principal component separately

Mann-Whitney U-Test log. vs. stat.	Mann-Whitney U	Z	Sig.	
PC1	15599	-17.054	0.000	*
PC2	55474	-2.141	0.032	*

A Mann-Whitney U-Test was performed to test for significant differences between the 2 groups along each principal component. According to these results, both growth phases significantly differed on each component (Table 3) due to their spectral composition.

Before performing PCA with spectra of treatments grown under various carbon concentrations, both growth phases were analyzed individually. Differences between clusters were again tested using a Mann-Whitney U-Test.

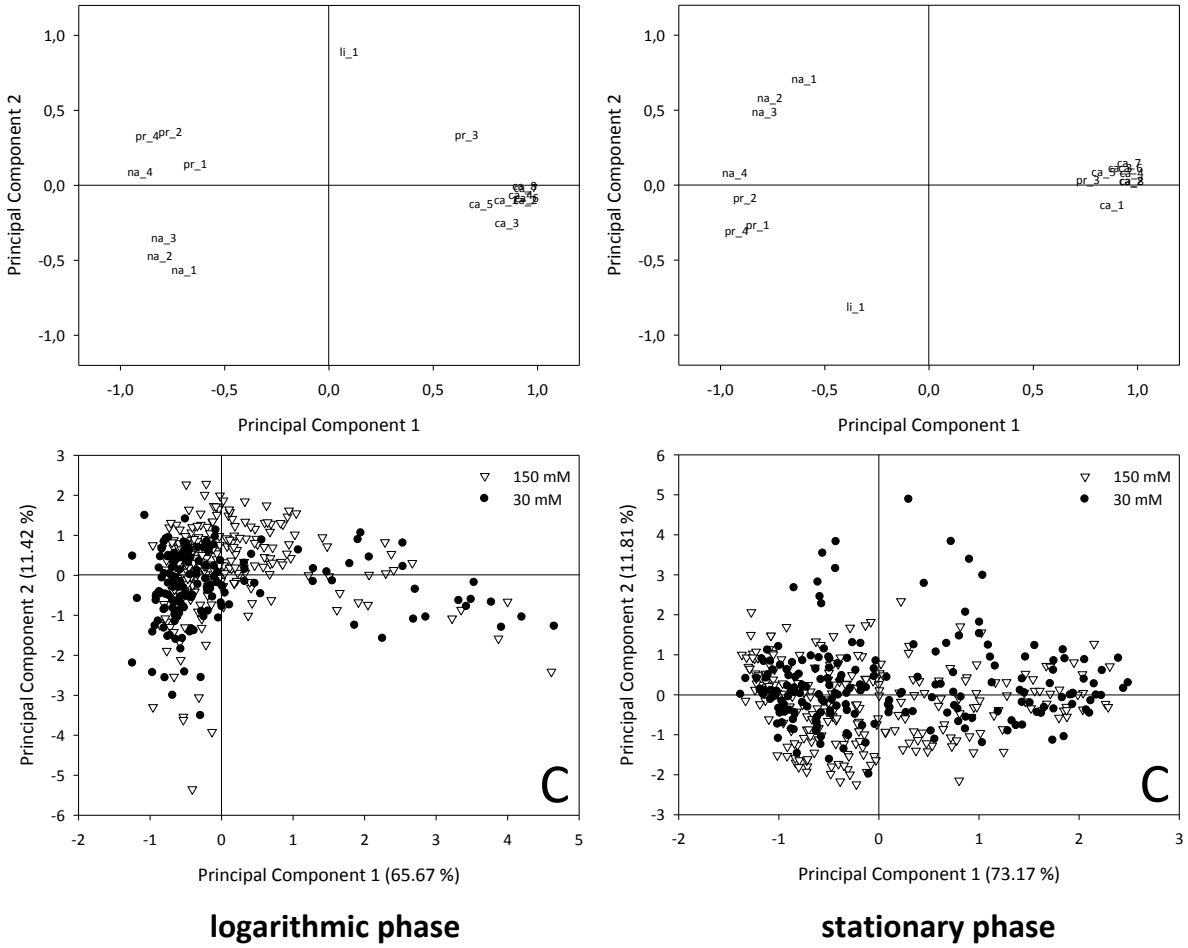

Figure 9: PCA plots (top: loading plots, bottom: score plots) for the first two extracted principal components at logarithmic phase and stationary phase, different symbols indicate different C concentrations

Although the distribution in the PCA score plots (Figure 9) illustrate only loose groupings the, statistical test results (Table 4) prove them to be significantly different in the logarithmic phase along PC1 and PC2, and in the stationary phase only on PC2.

Table 4: Results of Mann-Whitney U-Test comparing C-levels at each growth phase, test for significance was performed for each principal component separately

Mann-Whitney U-Test

C		Mann-Whitney U	Z	Sig.	
logarithmic	PC1	16319	-3.709	0.000	*
	PC2	13434	-6.097	0.000	*
stationary	PC1	22384	-1.217	0.224	
	PC2	19478	-3.405	0.001	*

Influences of varying N and P supply were further examined applying PCA to all spectra, which were subsequently defined and arranged corresponding to their resource N and P concentrations, and the N:P ratio. Figures 10 and 11 present the calculated loading plots and score plots for the two C-levels separately for each growth stage. The high C-level represents an initial carbon concentration of 150 mM whereas the low C-level corresponds to 30 mM. For three of these four considered categories two principal components could be extracted according to the Kaiser-criterion. An exception was the high C-level in the logarithmic phase, where it was five principal components.

The component loadings of the variables tend to be similar throughout all treatments. The carbohydrate signals load exceptionally consistent on the positive side of PC1, indicating similar behavior of the peaks. Though the peak named pr_3 could be identified as a protein signal it was consistently collocated with the carbohydrate peaks. Nucleic acid peaks and the remaining protein peaks could be located at the negative side of PC1. Both were differentiated through PC2 whereas nucleic acid peaks loaded on the positive and the proteins preferentially on the negative sector. As an exception, the low C treatments in the logarithmic phase resulted in a mirrored situation of the distribution. Here nucleic acid peaks loaded negatively and proteins positively. The peak referring to the lipid signal was found separated from the others and contributed mainly to PC2.

The individual spectra being contained in the plots were arranged according to their particular nutritional conditions. The obtained clusters differ in the extent of their dispersion, i.e. are more loosely or tightly grouped. To check whether it is possible to differentiate between these clusters, tests for equality of groups were performed. In this case, I consulted the Kruskal-Wallis H-Test for 3 or more groups (Table 5). If groups were identified as being significantly different, I additionally performed ANOVA post-hoc tests for

multiple comparisons after Games-Howell (Tables 6 and 7) since equal variances could not be assumed.

At the high C-level treatments situated in logarithmic growth phase, clusters grouped by N levels were significantly different only along PC1 ($P < 0.001$), both P-levels along PC2 ($P < 0.001$) and the three N:P-levels on both components (PC1: $P < 0.001$, PC2: $P < 0.001$). Low C-level treatments could be significantly separated by N-levels on PC1 ($P < 0.001$) and PC2 ($P < 0.05$) and by N:P-levels only on PC1 ($P < 0.001$). Here, P concentrations were not a discriminating criterion.

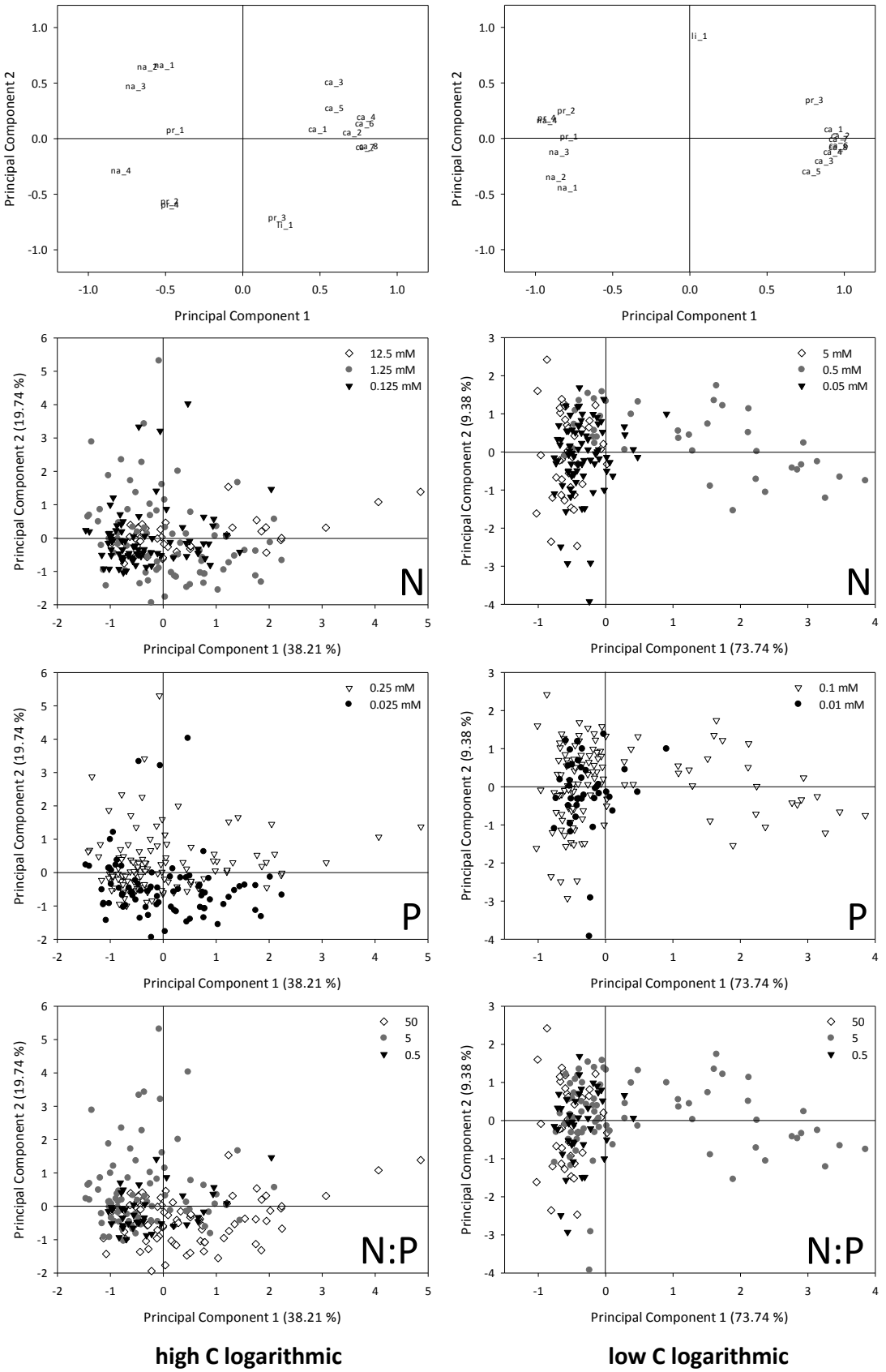

Figure 10: PCA loading and score plots for both C levels in the logarithmic growth phase. Treatments were arranged according to their elemental supply concentrations (N, P) and ratios (N:P)

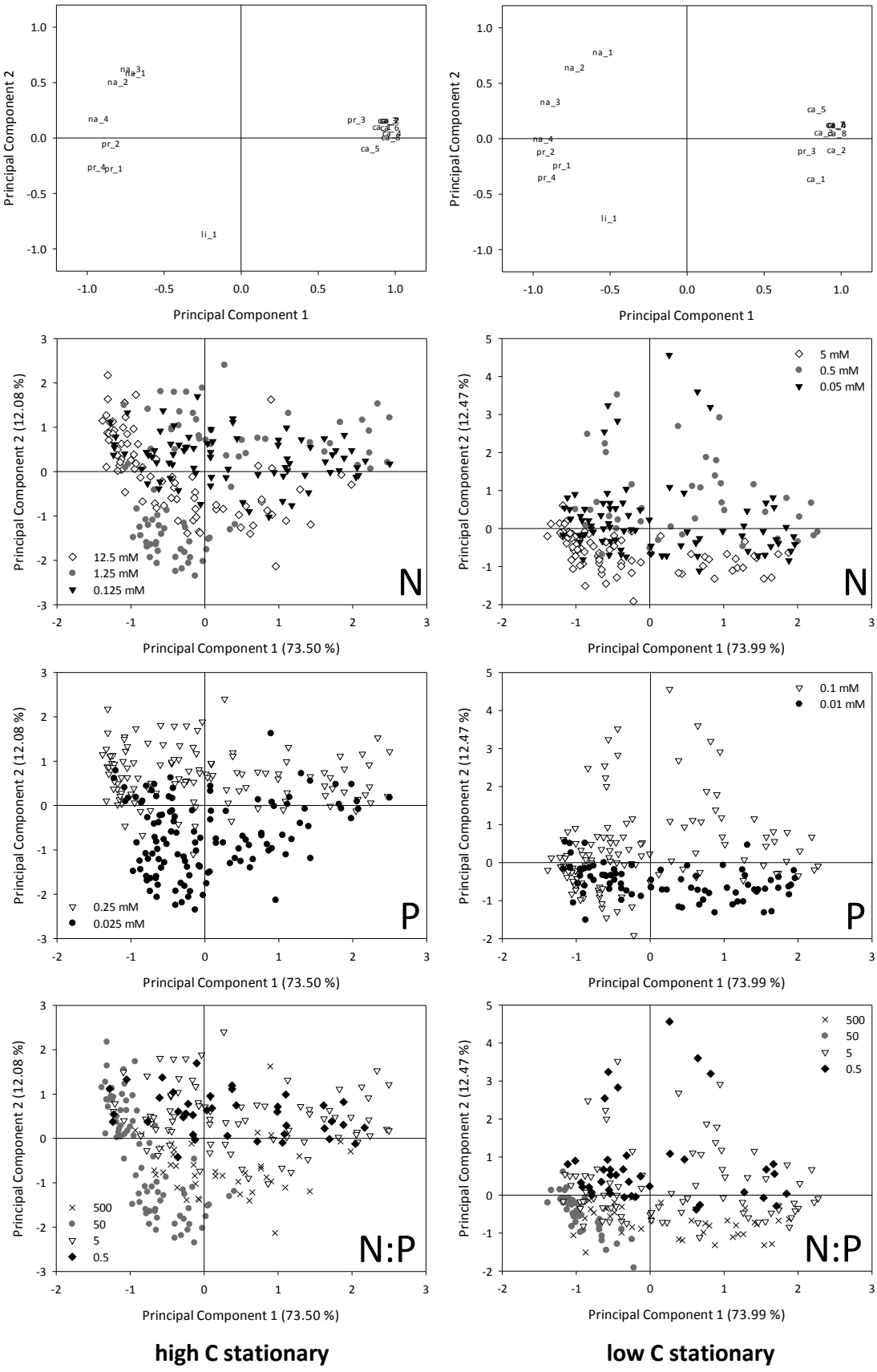

Figure 11: PCA loading and score plots at both C concentration levels separately in stationary phase. Treatments are arranged according to their elemental supply concentrations (N, P) and ratios (N:P)

At the high C-level in stationary phase different N concentrations lead to a significant discrimination on both components (PC1: $P < 0.05$, PC2: $P < 0.001$), whereas P concentrations discriminated among groups along PC2 ($P < 0.001$). N:P ratios significantly separated the treatments along PC1 ($P < 0.001$) and PC2 ($P < 0.001$).

At the low C concentrations in the stationary phase, N (PC1: $P < 0.001$, PC2: $P < 0.001$) and P (PC1: $P < 0.05$, PC2: $P < 0.001$) concentrations and N:P ratios (PC1: $P < 0.001$, PC2: $P < 0.001$) significantly differentiated clusters along both PC's.

Table 5: Results of tests for equality of treatments at different N, P or N:P levels along PC1 and PC2. Treatments have been separated into growth stages and C levels

Kruskal-Wallis H-Test					
N		Chi^2	df	Sig.	
high C logarithmic	PC1	18.461	2	0.000	*
	PC2	4.025	2	0.134	
low C logarithmic	PC1	65.253	2	0.000	*
	PC2	6.171	2	0.046	*
high C stationary	PC1	27.302	2	0.000	*
	PC2	7.901	2	0.019	*
low C stationary	PC1	25.775	2	0.000	*
	PC2	75.799	2	0.000	*
Mann-Whitney U-Test					
P		Mann-Whitney U	Z	Sig.	
high C logarithmic	PC1	4410	-0.973	0.331	
	PC2	2026	-6.918	0.000	*
low C logarithmic	PC1	2378	-0.087	0.931	
	PC2	2143	-1.013	0.311	
high C stationary	PC1	6360	-1.562	0.118	
	PC2	1221	-11.118	0.000	*
low C stationary	PC1	3784	-2.534	0.011	*
	PC2	1983	-7.025	0.000	*
Kruskal-Wallis H-Test					
N:P		Chi^2	df	Sig.	
high C logarithmic	PC1	39.037	2	0.000	*
	PC2	28.606	2	0.000	*
low C logarithmic	PC1	45.317	2	0.000	*
	PC2	1.618	2	0.445	
high C stationary	PC1	86.710	3	0.000	*
	PC2	62.445	3	0.000	*
low C stationary	PC1	59.402	3	0.000	*
	PC2	82.063	3	0.000	*

Table 6: Games-Howell multiple comparisons between groups of different elemental supply concentrations and ratios, * indicates significant differences between the respective groups compared to each other

high C – logarithmic

	N groups	N groups	Sig.	
PC1	12.5	1.25	0.157	
		0.125	0.001	*
	1.25	12.5	0.157	
		0.125	0.005	*
	0.125	12.5	0.001	*
		1.25	0.005	*
PC2	12.5	1.25	0.922	
		0.125	0.723	
	1.25	12.5	0.922	
		0.125	0.977	
	0.125	12.5	0.723	
		1.25	0.977	

	N:P groups	N:P groups	Sig.	
PC1	50	5	0.000	*
		0.5	0.000	*
	5	50	0.000	*
		0.5	0.483	
	0.5	50	0.000	*
		5	0.483	
PC2	50	5	0.000	*
		0.5	0.012	*
	5	50	0.000	*
		0.5	0.003	*
	0.5	50	0.012	*
		5	0.003	*

low C – logarithmic

	N groups	N groups	Sig.	
PC1	5	0.5	0.000	*
		0.05	0.000	*
	0.5	5	0.000	*
		0.05	0.000	*
	0.05	5	0.000	*
		0.5	0.000	*
PC2	5	0.5	0.143	
		0.05	0.955	
	0.5	5	0.143	
		0.05	0.019	*
	0.05	5	0.955	
		0.5	0.019	*

	N:P groups	N:P groups	Sig.	
PC1	50	5	0.000	*
		0.5	0.012	*
	5	50	0.000	*
		0.5	0.000	*
	0.5	50	0.012	*
		5	0.000	*
PC2	50	5	0.667	
		0.5	0.975	
	5	50	0.667	
		0.5	0.451	
	0.5	50	0.975	
		5	0.451	

Table 7: Games-Howell multiple comparisons between groups of different elemental supply concentrations and ratios, * indicates significant differences between the respective groups compared to each other

high C - stationary

	N groups	N groups	Sig.	
PC1	12.5	1.25	0.005	*
		0.125	0.000	*
	1.25	12.5	0.005	*
		0.125	0.143	
	0.125	12.5	0.000	*
		1.25	0.143	
PC2	12.5	1.25	0.407	
		0.125	0.019	*
	1.25	12.5	0.407	
		0.125	0.002	*
	0.125	12.5	0.019	*
		1.25	0.002	*

	N:P groups	N:P groups	Sig.	
PC1	500	50	0.000	*
		5	0.554	
		0.5	0.957	
	50	500	0.000	*
		5	0.000	*
		0.5	0.000	*
	5	500	0.554	
		50	0.000	*
		0.5	0.925	
	0.5	500	0.957	
		50	0.000	*
		5	0.925	
PC2	500	50	0.474	
		5	0.000	*
		0.5	0.000	*
	50	500	0.474	
		5	0.000	*
		0.5	0.000	*
	5	500	0.000	*
		50	0.000	*
		0.5	0.863	
	0.5	500	0.000	*
		50	0.000	*
		5	0.863	

low C- logarithmic

	N groups	N groups	Sig.	
PC1	5	0.5	0.000	*
		0.05	0.008	*
	0.5	5	0.000	*
		0.05	0.114	
	0.05	5	0.008	*
		0.5	0.114	
PC2	5	0.5	0.000	*
		0.05	0.000	*
	0.5	5	0.000	*
		0.05	0.027	*
	0.05	5	0.000	*
		0.5	0.027	*

	N:P groups	N:P groups	Sig.	
PC1	500	50	0.000	*
		5	0.926	
		0.5	0.737	
	50	500	0.000	*
		5	0.000	*
		0.5	0.000	*
	5	500	0.926	
		50	0.000	*
		0.5	0.282	
	0.5	500	0.737	
		50	0.000	*
		5	0.282	
PC2	500	50	0.251	
		5	0.000	*
		0.5	0.000	*
	50	500	0.251	
		5	0.000	*
		0.5	0.000	*
	5	500	0.000	*
		50	0.000	*
		0.5	0.031	*
	0.5	500	0.000	*
		50	0.000	*
		5	0.031	*

Discussion

Intracellular macromolecular composition

This study was conducted to examine whether different concentrations and ratios of elemental C, N and P supply result in varying uptake and especially how this nutritional variance affects the subsequent assembly of the three cellular key constituents, such as carbohydrates, proteins and nucleic acids. As these macromolecules are known to differ considerably in their elemental composition, it was reasonable to use them as indicators to discern effects of resource stoichiometry. Consequently, the intracellular composition of *V. spinosum* from the various stoichiometric treatments had to be measured efficiently and in a reproductive way. Additionally, I decided not to look for effects particularly on the constitution of the harvested bulk biomass but to use a method for analyzing influences on single cells.

Raman spectroscopy emerged to be an appropriate tool based on the ability to measure relative quantities of intracellular compounds on this requested high level of resolution (Schuster et al. 2000, Huang et al. 2004). Several compounds could be tentatively assigned to the detected spectral peaks according to data reported in the literature (Goral & Zichy 1990, Schuster et al. 2000, Maquelin et al. 2002, De Gelder et al. 2007b). Unfortunately, substantial information on the macromolecular composition in the Raman spectra of bacterial cells remained still poorly assignable. For instance, the peak pr_3 referred to as a protein peak (Kneipp et al. 2006) behaved similarly as did carbohydrate peaks in all PCA analyses. However, to conform to the literature, I retained the pr_3 peak as a protein signal.

The complexity of the acquired data necessitated the processing including baseline correction, normalization and smoothing of the raw-spectra. Hence, I could not precisely determine absolute concentrations as could be demonstrated in an earlier approach (Giles et al. 1999). In these studies, Raman spectroscopy was used to measure concentrations of pure chemical solutions at a high linearity level and precision. However, to detect and understand changes in selected macromolecules between the growth phases and among resource stoichiometries, absolute concentrations are not required.

The logarithmic growth phase of a bacterial population in batch cultures is defined as the time where bacteria maintain elevated metabolism and exponential population growth (Buchanan 1918). This is followed by the stationary phase where cell division decelerates

and metabolism becomes reduced with cells persisting in a vegetative state for extended periods.

Spectral analysis of these two phases revealed distinct changes in the cellular macromolecular composition as illustrated by the stoichiometric resource treatment #6 (C:N:P 6000:5:1, Figure 1). Peaks indicative of carbohydrates generally suggested an increase of the cellular carbohydrate content during the stationary phase. These peaks largely contribute to carbohydrate pools related to intracellular storage of carbon, such as polysaccharides and possibly polyhydroxyalkanoates (PHA). The latter are known as being synthesized in a fermentative pathway and deposited as insoluble inclusions in the cytoplasm. This occurs in most bacteria, particularly if cultivated in excess of carbon and if growth is simultaneously impaired or restricted by the scarcity of nutrients (e.g. N or P) (Madison & Huisman 1999). Previous Raman analyses of bacteria producing poly (3-hydroxybutyrates) (PHB) (De Gelder et al. 2008) determined the assignation of respective signals to some carbohydrate peaks I was able to detect in stationary spectra of *Verrucomicrobium spinosum*. These peaks imply the wavenumber regions of 854 cm^{-1}, 936 cm^{-1} and 1030-1130 cm^{-1}.

Proteins, as the main nitrogen repositories, were characterized by four different peaks. The phenylalanine signal (pr_1) was considered to be one of them, since this proteinogenic amino acid is the only one able to be identified precisely in bacterial Raman spectra. Reaching stationary phase the protein peaks pr_1, pr_2 and pr_4 decreased whereas pr_3 increased. These observations indicate the intracellular protein configuration to be affected by the changing metabolism during the transition from logarithmic to stationary growth phase. The degradation and assembling of different protein types confirm a reorganization of the protein composition also due to an evolving demand of stress resistance, e.g. because of nutrient depletion.

Peaks assigned to nucleic acids primarily decreased after the transition to stationary phase. This confirms assumptions (Poulsen et al. 1993) on the degradation of rRNA during growth inhibition or starvation. Although newer surveys established the relationship of metabolic rate and rRNA content to break apart at very high and very low growth rates (Schmid et al. 2001) my results tend to confirm the correlation.

One goal of this study was to test bacterial Raman spectroscopy as a convenient tool to measure cellular macromolecular concentrations. For this purpose, I could not associate

Raman-derived values with concentrations derived from alternative techniques — simply because they were not available. Therefore, I correlated Raman-derived values indicative of macromolecular concentration with measurements of the bulk biomass.

As illustrated in Figures 2 – 4, Raman signals are suitable to reflect different intracellular concentrations of carbohydrates, proteins and nucleic acids governed by the different signal strengths. Acquired values are just loosely related to bulk biomass measurements. Comparing fluorometrically measured nucleic acid concentrations from entire cell pellets and Raman signals from single cells revealed good correlations in logarithmic yet not in the stationary phase.

I found clear responses of the macromolecular concentration to the biomass stoichiometry. An increasing C:N ratio is linked to both an increase in carbohydrates and a decline in the level of proteins. These relationships are evident since increasing concentrations of carbohydrates require additional carbon. The separation in different growth phases confirms that bacteria in stationary phase tend to incorporate more carbohydrates than bacteria in logarithmic phase. An increase in nitrogen, reflecting a decrease of the C:N ratio, was shown to produce higher protein signals, and the division of both growth phases indicates that bacteria entering the stationary phase tend to decrease their protein content.

The fact that nucleic acids constitute the major fraction of the cellular P suggests that varying nucleic acid content should produce considerable variation in C:P ratios. *V. spinosum* showed different behavior under high and low P supply. Classifying the data points in Figure 7 according to their respective P level reveals that the correlation at low P treatments supports this simple assumption. At a high P supply, the nucleic acid content could not explain any variance in biomass C:P. I suggest that this decoupling of the relationship is mediated by an increased uptake rate due to the high external P concentration. As a consequence, these high loads of P exceed the demand of nucleic acid allocation or other growth requirements and are therefore deposited in storage pools most likely consisting of inorganic polyphosphates. Such luxury consumption (Sterner & Elser 2002) occurs when a different factor (e.g. another nutrient) limits growth and the uptake of the non-limiting nutrient continues.

PCA analyses clearly discriminated both growth phases based on the selected peaks from the Raman spectra (Figure 8). Additionally, both growth phases varied considerably in their

distributional pattern. The logarithmic phase cluster displayed a more constricted scatter, only slightly expanded along PC2 due to the spacing between nucleic acid peaks and protein peaks 1, 2 and 4 in the loading plot. The cluster indicating the stationary growth phase stretches across the entire PC1 driven by a pronounced heterogeneity of the spectral constitutions among different treatments as well as among cells of the same treatment. This wide-spreading effect is particularly due to the contribution of the carbohydrate peaks. I assume this occurs as the different treatments enter stationary phase after depleting some of the nutrients. Since they differ in their supply mixture other nutrients, or carbon in this case, might still be available and the bacteria excessively consume them and form appropriate storage compounds. Bacteria of treatments supplying high N or P resources demonstrated to contain themselves higher amounts of protein and nucleic acids, respectively. This effect obviously indicates a certain degree of flexibility of their physiology corresponding to the available nutrients. As another issue causing the observed heterogeneity may be considered the fact that cells in stationary phase appear in various physiological states. Generally, a major part of the variation in the data set (up to 74%) was explained by PC1.

For practical purposes, both growth phases were subsequently explored apart from each other. The significant divergence of the two provided C concentrations along both principal components (Figure 9) revealed a substantial influence of carbohydrates, proteins and nucleic acids during logarithmic phase. Some samples with high positive loadings on PC1, producing a dispersed expansion, suggest that there exist spectra dominated by carbohydrate signals and the cells are therefore expected to already having entered early stationary phase. The analysis of stationary phase samples again pictures a very heterogeneous distribution. The formation of distinct clusters according to the carbon levels could not be proved to be significant on PC1. But even though PC2 is just responsible for 11.8% of the variation it can be accounted for a significant separation of the groupings. But this might be indicative for carbon being only a marginal factor influencing the diversity of spectral patterns in stationary phase.

Breaking up the C levels was necessary to obtain information about the role of N, P and their ratio (Figures 10 & 11). At a high C concentration in logarithmic phase the nitrogen level might have influenced the assembling of proteins in bacteria. The Games-Howell multiple comparisons (Table 5) indicate a breakup of the low N cluster from the remaining mid- and

high N groups due to a less intense allocation of proteins as illustrated by the corresponding loading plot. As production of carbohydrates may be just indirectly affected by the supply nitrogen level their influence should just have minor relevance. Much more explicit is the impact of the P supply on the spectral pattern. A greater external reserve of available P results in a higher yield of nucleic acid production. P might also be the primary player influencing the effect of N:P on the intracellular composition. Whereas there is no difference between N:P ratios of 0.5 and 5, the higher ratio of 50 enforces the cells to produce more proteins relative to nucleic acids. At low carbon concentrations PCA generated once more separated groups according to the varying N supply which in this case only spread significantly along PC1. Samples of treatment #9 (C:N:P 300:5:1) surprisingly extended the distribution towards the positive region of PC1, indicating elevated cellular carbohydrates. A reasonable explanation for this effect could not be found yet. P seems not to be an influencing factor on the macromolecular composition at this C level and growth phase. The supply N:P ratio pretends to influence the cell's composition, but again treatment #9 (C:N:P 300:5:1) avoids a distinct interpretation.

Treatments cultivated at 150mM C until stationary phase were also affected by varying N and P conditions. High N (12.5 mM) and high P (0.25 mM) concentrations induced the production of higher nucleic acid quantities. Reducing only the P-level resulted in assembling more proteins whereas a decrease in N forced the cells to invest in carbohydrates. The distribution of clusters affected by the N:P ratio supports this association. High N:P ratios (500, 50) raise the tendency to assemble more intracellular proteins. Lower N:P ratios (5, 0.5) generated an extended nucleic acid and carbohydrate content. The fact that at a C level of 30 mM the treatments behaved similarly under comparable N and P concentrations suggests that carbon might not have a determining influence on the spectral composition in stationary phase and approves the already mentioned assumption.

Synthesis

I unveiled Raman spectroscopy as an instrument to better understand biomass stoichiometry at cell level. It is applicable to cells grown at different nutrient concentrations and enables rapid insight in the cell's macromolecular composition at any phase of growth. This may in future research help to easily realize biological functions as a consequence of the macromolecular and nutritional demand and allows insight into the physiological

constraints. The striking benefit is the applicability on a never before achieved single cell level and is therefore in addition to different molecular tools able to infiltrate bacterial communities (Huang et al. 2007) and dissipate not just single species but single bacteria at different physiological modes. To develop its maximum potential there is more insight into the hidden spectral information needed. Being able to identify also phospholipid- and polyphosphate signals or signals of inorganic N-storage compounds etc. may help to explain a greater proportion of the implied variation.

Acknowledgments

I wish to thank Tom Battin for his formal supervision and enduring patience over the entire period of my work. I am also thankful to the Department of Microbial Ecology (University of Vienna) for providing the Raman equipment and hospitality in their laboratories and especially Kilian Stoecker and Frank Maixner for supplying theoretical and technical advice. Furthermore, I need to thank Margarete Watzka for the C and N, Katharina Keiblinger for the P, Christian Preiler for the protein and carbohydrate analyses and Ieda Nunez Hämmerle for easing the work of cultivating *V. spinosum*. I am deeply grateful to Gabriel Singer and Christian Baranyi for guiding me through the difficulties of statistical procedures. Special acknowledgments deserve Christian Schwarz and Edward K. Hall for their continuous inventive input, advices and support. Funding for this research came from the MICDIF project (FWF).

Literature cited

Bradford MM (1976) Rapid and Sensitive Method for Quantitation of Microgram Quantities of Protein Utilizing Principle of Protein-Dye Binding. Analytical Biochemistry 72:248-254

Buchanan RE (1918) Life phases in a bacterial culture. Journal of Infectious Diseases 23:109-125

Daniels L, Hanson RS, Phillips J (2007) Total Carbohydrates by Phenol Reaction. In: Reddy CA, Beveridge, T.J., Breznak, J.A., Marzluf, G.A., Schmidt, T.M., and L.R. Snyder (ed) Methods for General and Molecular Microbiology, 3rd Ed. Section III: Chemical Analysis ASM Press
Washington, DC, p 468

De Gelder J, De Gussem K, Vandenabeele P, De Vos P, Moens L (2007a) Methods for extracting biochemical information from bacterial Raman spectra: An explorative study on Cupriavidus metallidurans. Analytica Chimica Acta 585:234-240

De Gelder J, De Gussem K, Vandenabeele P, Moens L (2007b) Reference database of Raman spectra of biological molecules. Journal of Raman Spectroscopy 38:1133-1147

De Gelder J, Willemse-Erix D, Scholtes M, Sanchez J, Maquelin K, Vandenabeele P, De Boever P, Puppels G, Moens L, De Vos P (2008) Monitoring Poly (3-hydroxybutyrate) Production in Cupriavidus necator DSM 428 (H16) with Raman Spectroscopy. Anal. Chem 80:2155-2160

Dodds WK, Marti E, Tank JL, Pontius J, Hamilton SK, Grimm NB, Bowden WB, McDowell WH, Peterson BJ, Valett HM, Webster JR, Gregory S (2004) Carbon and nitrogen stoichiometry and nitrogen cycling rates in streams. Oecologia 140:458-467

Escoriza MF, Vanbriesen JM, Stewart S, Maier J (2006) Studying bacterial metabolic states using Raman spectroscopy. Appl Spectrosc 60:971-976

Giles J, Gilmore D, Denton M (1999) Quantitative analysis using Raman spectroscopy without spectral standardization. Journal of Raman Spectroscopy 30:767-771

Goodacre R, Timmins EM, Burton R, Kaderbhai N, Woodward AM, Kell DB, Rooney PJ (1998) Rapid identification of urinary tract infection bacteria using hyperspectral whole-organism fingerprinting and artificial neural networks. Microbiology-Sgm 144:1157-1170

Goral J, Zichy V (1990) Fourier-Transform Raman Studies of Materials and Compounds of Biological Importance. Spectrochimica Acta Part a-Molecular and Biomolecular Spectroscopy 46:253-275

Hanlon EB, Manoharan R, Koo TW, Shafer KE, Motz JT, Fitzmaurice M, Kramer JR, Itzkan I, Dasari RR, Feld MS (2000) Prospects for in vivo Raman spectroscopy. Physics in Medicine and Biology 45:R1-R59

Hessen DO, Agren GI, Anderson TR, Elser JJ, Ruiter PCd (2004) Carbon Sequestration in Ecosystems: The Role of Stoichiometry. Ecology 85:1179-1192

Huang WE, Griffiths RI, Thompson IP, Bailey MJ, Whiteley AS (2004) Raman microscopic analysis of single microbial cells. Analytical Chemistry 76:4452-4458

Huang WE, Stoecker K, Griffiths R, Newbold L, Daims H, Whiteley AS, Wagner M (2007) Raman-FISH: combining stable-isotope Raman spectroscopy and fluorescence in situ hybridization for the single cell analysis of identity and function. Environmental Microbiology 9:1878-1889

Hutsebaut D, Vandroemme J, Heyrman J, Dawyndt P, Vandenabeele P, Moens L, de Vos P (2006) Raman microspectroscopy as an identification tool within the phylogenetically homogeneous 'Bacillus subtilis' group. Syst Appl Microbiol 29:650-660

Jarvis RM, Goodacre R (2004) Discrimination of bacteria using surface-enhanced Raman spectroscopy. Analytical Chemistry 76:40-47

Kirschner C, Maquelin K, Pina P, Ngo Thi NA, Choo-Smith LP, Sockalingum GD, Sandt C, Ami D, Orsini F, Doglia SM, Allouch P, Mainfait M, Puppels GJ, Naumann D (2001) Classification and identification of enterococci: a comparative phenotypic, genotypic, and vibrational spectroscopic study. J Clin Microbiol 39:1763-1770

Kneipp J, Kneipp H, McLaughlin M, Brown D, Kneipp K (2006) In vivo molecular probing of cellular compartments with gold nanoparticles and nanoaggregates. Nano Letters 6:2225-2231

Lopez-Diez EC, Goodacre R (2004) Characterization of microorganisms using UV resonance Raman spectroscopy and chemometrics. Analytical Chemistry 76:585-591

Madison LL, Huisman GW (1999) Metabolic engineering of poly(3-hydroxyalkanoates): From DNA to plastic. Microbiology and Molecular Biology Reviews 63:21-+

Makino W, Cotner JB (2004) Elemental stoichiometry of a heterotrophic bacterial community in a freshwater lake: implications for growth- and resource-dependent variations. Aquatic Microbial Ecology 34:33-41

Makino W, Cotner JB, Sterner RW, Elser JJ (2003) Are bacteria more like plants or animals? Growth rate and resource dependence of bacterial C : N : P stoichiometry. Functional Ecology 17:121-130

Manzoni S, Jackson RB, Trofymow JA, Porporato A (2008) The global stoichiometry of litter nitrogen mineralization. Science 321:684-686

Maquelin K, Kirschner C, Choo-Smith LP, van den Braak N, Endtz HP, Naumann D, Puppels GJ (2002) Identification of medically relevant microorganisms by vibrational spectroscopy. Journal of Microbiological Methods 51:255-271

McKee KL, Feller IC, Popp M, Wanek W (2002) Mangrove isotopic (delta N-15 and delta C-13) fractionation across a nitrogen vs. phosphorus limitation gradient. Ecology 83:1065-1075

Naumann D, Keller S, Helm D, Schultz C, Schrader B (1995) Ft-Ir Spectroscopy and Ft-Raman Spectroscopy Are Powerful Analytical Tools for the Noninvasive Characterization of Intact Microbial-Cells. Journal of Molecular Structure 347:399-405

Oust A, Moretro T, Naterstad K, Sockalingum GD, Adt I, Manfait M, Kohler A (2006) Fourier transform infrared and raman spectroscopy for characterization of Listeria monocytogenes strains. Appl Environ Microbiol 72:228-232

Poulsen L, Ballard G, Stahl D (1993) Use of rRNA fluorescence in situ hybridization for measuring the activity of single cells in young and established biofilms. Applied and Environmental Microbiology 59:1354-1360

Schinner F, Öhlinger R, Kandeler E, Margesin R (1993) Bodenbiologische Arbeitsmethoden.

Schlesner H (1987) Verrucomicrobium-Spinosum Gen-Nov, Sp-Nov - a Fimbriated Prosthecate Bacterium. Systematic and Applied Microbiology 10:54-56

Schlesner H (1994) The Development of Media Suitable for the Microorganisms Morphologically Resembling Planctomyces Spp, Pirellula Spp, and Other Planctomycetales from Various Aquatic Habitats Using Dilute Media. Systematic and Applied Microbiology 17:135-145

Schmid M, Schmitz-Esser S, Jetten M, Wagner M (2001) 16S-23S rDNA intergenic spacer and 23S rDNA of anaerobic ammonium-oxidizing bacteria: implications for phylogeny and in situ detection. Environmental Microbiology 3:450-459

Schrader B, Dippel B, Erb I, Keller S, Lochte T, Schulz H, Tatsch E, Wessel S (1999) NIR Raman spectroscopy in medicine and biology: results and aspects. Journal of Molecular Structure 481:21-32

Schuster KC, Reese I, Urlaub E, Gapes JR, Lendl B (2000) Multidimensional information on the chemical composition of single bacterial cells by confocal Raman microspectroscopy. Analytical Chemistry 72:5529-5534

Sterner RW, Elser JJ (2002) Ecological stoichiometry : the biology of elements from molecules to the biosphereedn. Princeton University Press, Princeton

Tezuka Y (1990) Bacterial Regeneration of Ammonium and Phosphate as Affected by the Carbon : Nitrogen : Phosphorus Ratio of Organic Substrates. Microbial Ecology 19:227-238

Watzka M, Buchgraber K, Wanek W (2006) Natural N-15 abundance of plants and soils under different management practices in a montane grassland. Soil Biology & Biochemistry 38:1564-1576

Anhang

Zusammenfassung

Die ökologische Stöchiometrie bietet eine Grundlage zur Beschreibung der Bilanz mehrerer chemischer Elemente in ökologischen Wechselbeziehungen. Auf Basis der Konzepte von Sterner & Elser (2002) können so Verbindungen zwischen der Funktion, Physiologie und der elementaren Zusammensetzung, vor allem von Kohlenstoff (C), Stickstoff (N) und Phosphor (P), eines Organismus gezogen werden. Zum Verständnis komplexer Funktionen diverser Gemeinschaftsstrukturen habe ich versucht diese zu zerlegen, indem Einflüsse unterschiedlicher Nährstoffversorgung auf die Physiologie eines einzelnen Bakterienstammes, *Verrucomicrobium spinosum,* untersucht wurden. In diesem Zusammenhang stelle ich einen auf dem Gebiet neuartigen Ansatz vor, basierend auf der Möglichkeit mittels Raman Mikrospektroskopie makromolekulare Bestandteile auf zellulärer Ebene zu messen. Seine Vorteile ermöglichten einen detaillierten Einblick in den Zusammenhang zwischen dem C, N und P Angebot und dessen Zuordnung in zelluläre Biomoleküle, wie zum Beispiel in Kohlenhydrate, Proteine und Nukleinsäuren. Die Aufgabe bestand zuerst aus der Kultivierung von *V. spinosum* in Batch-Kulturen unter 12 verschiedenen Nährstoffbedingungen. Anschließend wurden die Bakterien an zwei vorher festgelegten Zeitpunkten geerntet. Diese sollten zur Beprobung der logarithmischen und stationären Wachstumsphase dienen, um auch auf wachstumsbedingte Auswirkungen auf die Zusammensetzung zu prüfen.

Spektrale Aufnahmen von *Verrucomicrobium spinosum* in der logarithmischen Wachstumsphase zeigten sehr ähnliche intrazelluläre Muster der makromolekularen Zusammensetzung, nur wenig beeinflusst von den unterschiedlichen Nährstoffkonzentrationen im umliegenden Medium. Dies lässt auf einen hohen Grad an physiologischer Homöostase schließen. In der stationären Phase stellte sich heraus, dass sich Zellen aus Kulturen verschiedener Nährstoffbedingungen in der Zusammensetzung sehr stark unterschieden. Diese hier ausgebildete intrazelluläre Heterogenität wurde durch eine auf die vorliegende nährstoffliche Situation, die in diesem Wachstumsstadium schon durch Limitierungen geprägt werden kann, angepasste Physiologie bedingt.

Die mittels Raman Spektroskopie gemessenen Konzentrationen von Kohlenhydraten, Proteinen und Nukleinsäuren auf zellulärer Ebene ergaben repräsentative Werte, die mit traditionellen nasschemischen Methoden, angewendet auf größere Biomassen, zu einem gewissen Grad übereinstimmten.

Die gemessenen Konzentrationen dieser drei Komponenten konnten signifikant mit den C:N und C:P Verhältnissen in der Biomasse in Verbindung gebracht werden. Dadurch bestätigt sich die Annahme, dass diese drei Molekülgruppen, hauptsächlich bestehend aus C, N und P, jedoch zu unterschiedlichen Mengen, die wesentlichen Bestandteile in der Zelle ausmachen.

Unter Verwendung der Hauptkomponentenanalyse konnten wesentliche Auswirkungen von N und P auf die Anreicherung zellulärer Bestandteile nachgewiesen werden, wobei die Versorgung mit C offensichtlich keinen Einfluss auf die Speichermenge der Kohlenhydrate nahm. Dies bedeutet, dass auch das Vorhandensein von niedrigen C Konzentrationen in den Kulturen in jeder Phase ausreichend Ressourcen angeboten hat.

Zusammenfassend ist der angewandte methodische Ansatz imstande, relevante Verbesserungen in der Auffassung von Einflüssen, bedingt durch Ressourcen-Stöchiometrie, auf die mikrobielle Physiologie und im Weiteren auf ökosystemare Funktionen zu erbringen.

Lebenslauf

Persönliche Daten

Marvin Pölzl
Arndtstraße 21-23/3/5/13
A - 1120 Wien
Tel.: +43 660/3411800
Email: marvin.poelzl@gmail.com

Geburtsdaten:	Wien, 15. Dezember 1983
Staatsangehörigkeit:	Österreich
Familienstand:	ledig

Bildungsweg

WS 2004 – WS 2008	Diplomstudium der Biologie an der Universität Wien im Studienzweig Ökologie mit Spezialisierung auf Limnologie (2. Abschnitt)
WS 2002 – SS 2004	Diplomstudium der Biologie an der Universität Wien (1. Abschnitt)
17. Juni 2002	Reifeprüfung
1994 – 2002	AHS Erlgasse 32-34, 1120 Wien, ab 1998 Oberstufe im Realgymnasium
1990 – 1994	Volkschule Haebergasse 1A, 1120 Wien

Berufliche Erfahrung/Praktika

10/2008 – 11/2008	***Universität Wien*** Wissenschaftlicher Mitarbeiter im Rahmen des Projektes „Resource Limitation of microbial decomposition of soil organic matter“ am Department für Chemische Ökologie und Ökosystemforschung
04/2008 – 09/2008	***Universität Wien*** Wissenschaftlicher Mitarbeiter im Rahmen des Projektes „MICDIF“ am Department für Chemische Ökologie und Ökosystemforschung
10/2006 – 04/2007	***Universität Wien*** Wissenschaftlicher Mitarbeiter des Projektes „Flussbauliches Gesamtprojekt“
07/2006	***MA 45 – Wiener Gewässer***

	Praktikum
07/2005	***Tiergarten Schönbrunn***
	Praktikum als Tierhilfspfleger

Zusätzliche Kenntnisse und Fertigkeiten

Fremdsprachen	Englisch:	in Wort und Schrift
	Französisch:	Grundkenntnisse
Computerkenntnisse	Microsoft Office	
	SPSS, JMP 7, SigmaPlot	

Wien, im Jänner 2009